Developmental Cell
Article

Kinetochores Generate Microtubules with Distal Plus Ends: Their Roles and Limited Lifetime in Mitosis

Etsushi Kitamura,[1,4] Kozo Tanaka,[1,2,4] Shinya Komoto,[1,4] Yoko Kitamura,[1] Claude Antony,[3] and Tomoyuki U. Tanaka[1,*]
[1]Wellcome Trust Centre for Gene Regulation & Expression, University of Dundee, Dundee DD1 5EH, UK
[2]Institute of Development, Aging and Cancer, Tohoku University, Sendai 980-8575, Japan
[3]European Molecular Biology Laboratory, D-69117 Heidelberg, Germany
[4]These authors contributed equally to this work
*Correspondence: t.tanaka@lifesci.dundee.ac.uk
DOI 10.1016/j.devcel.2009.12.018

SUMMARY

In early mitosis, microtubules can be generated at kinetochores as well as at spindle poles. However, the role and regulation of kinetochore-derived microtubules have been unclear. In general, metaphase spindle microtubules are oriented such that their plus ends bind to kinetochores. However, we now have evidence that, during early mitosis in budding yeast, microtubules are generated at kinetochores with distal plus ends. These kinetochore-derived microtubules interact along their length with microtubules that extend from a spindle pole, facilitating kinetochore loading onto the lateral surface of spindle pole microtubules. Once kinetochores are loaded, microtubules are no longer generated at kinetochores, and those that remain disappear rapidly and do not contribute to the metaphase spindle. Stu2 (the ortholog of vertebrate XMAP215/ch-TOG) localizes to kinetochores and plays a central role in regulating kinetochore-derived microtubules. Our work provides insight into microtubule generation at kinetochores and the mechanisms that facilitate initial kinetochore interaction with spindle pole microtubules.

INTRODUCTION

Microtubules (MTs) are cytoskeletal filaments composed of α-β-tubulin heterodimers. MTs have intrinsic polarity, defined by the orientation of tubulin heterodimers, and show different dynamics at opposite ends: plus ends are more dynamic, with tubulin dimers being polymerized and depolymerized, whereas minus ends are either static or only undergo depolymerization (Dammermann et al., 2003; Howard and Hyman, 2003).

The mitotic spindle comprises MTs emanating from spindle poles and plays pivotal roles in chromosome segregation during mitosis (Walczak and Heald, 2008). The forces required for chromosome segregation are mainly generated by MTs that connect kinetochores (KTs) to spindle poles (KT-spindle pole MTs). There was a long-standing debate concerning the origin of KT-spindle pole MTs (Rieder, 2005).

In the 1970s, several studies demonstrated that KTs on isolated chromosomes could generate MTs in vitro (e.g., McGill and Brinkley, 1975) and suggested that KT-derived MTs have their plus ends distal to KTs (Bergen et al., 1980; Summers and Kirschner, 1979). It was also found that after removal of MT-polymerization inhibitors, MTs extend from KTs in mammalian cells (e.g., Witt et al., 1980). However, by that time, it was also clear that spindle poles have potent activity for generating MTs with distal plus ends; thus, it was unclear whether the MTs that eventually mediate the KT-spindle pole connection are derived from the spindle poles or the KTs.

A clear answer emerged when the polarity of KT-spindle pole MTs was determined. An in situ MT polarity assay established that during metaphase all KT-spindle pole MTs have their plus ends at KTs, not at spindle poles (McIntosh and Euteneuer, 1984). Thus, it was concluded that KT-spindle pole MTs mainly originate from spindle poles, not from KTs. Consolidating this conclusion, it was also shown that KTs indeed capture MTs from spindle poles (spindle pole MTs) in early mitosis (Kirschner and Mitchison, 1986; Rieder and Alexander, 1990).

KT interactions with spindle pole MTs develop in a stepwise manner. At the start of mitosis, KTs initially interact with the lateral surface of spindle pole MTs (Rieder and Alexander, 1990; Tanaka et al., 2005). Then, MTs that extend from the other spindle pole also interact with KTs. Finally, sister KTs attach to the ends of MTs that extend from opposite poles (sister KT biorientation) before anaphase onset (Tanaka, 2008). These processes and mechanisms are well conserved from yeast to vertebrate cells.

Although KT-spindle pole MTs mainly originate from spindle poles, KT-derived MTs contribute to the formation of KT-spindle pole MTs in some organisms. For example, in *Drosophila* cells, MTs with distal minus ends sometimes extend from KTs, subsequently being tethered at spindle poles (Khodjakov et al., 2003; Maiato et al., 2004). Intriguingly, in these studies, the polarity of KT-derived MTs was opposite to what was suggested in the 1970s (see above). It remained unclear whether the generation of MTs at KTs with distal plus ends, reported in the 1970s, was an in vitro artifact or had any physiological relevance.

Another enigma surrounding KT-MT interactions is the efficiency with which spindle pole MTs are able to "locate" KTs

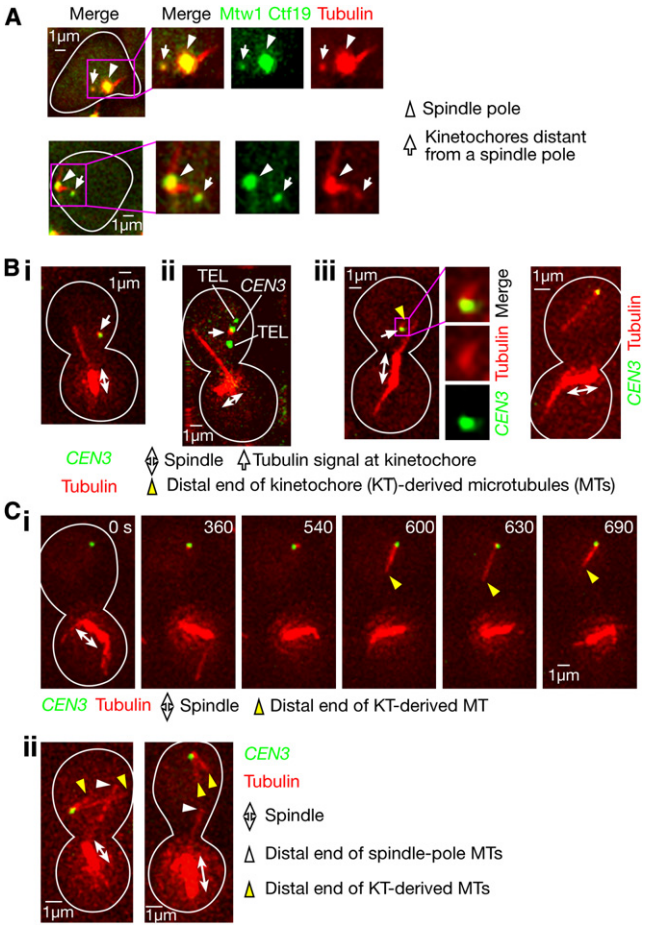

Figure 1. Microtubules Are Generated at Kinetochores prior to Their Interaction with Spindle Pole Microtubules

(A) Tubulin signals are found at reassembled KTs before their interaction with spindle pole MTs in S phase. *CTF19-3×GFP MTW1-3×GFP YFP-TUB1* cells (T3110) were treated with α factor and subsequently released to fresh media. After 25 min, YFP (tubulin; red) and GFP (Ctf19, Mtw1; green) images were acquired. Cell shapes are outlined in white.

(B) Tubulin signals are found at *CEN3* after its reactivation and showed extension in some cases. (i and iii) P_{GAL}-*CEN3-tetOs* (replacing *CEN3*) *TetR-3×CFP YFP-TUB1* P_{MET3}-*CDC20* cells (T3828) were treated with α factor in methionine drop-out medium with raffinose for 2.5 hr, and then released to YP medium containing galactose, raffinose, and 2 mM methionine. After 3.5 hr, cells were suspended in synthetic complete medium containing glucose and methionine. Subsequently, YFP (tubulin; red) and CFP (*CEN3*; green) images were acquired. (ii) P_{GAL}-*CEN3-tetOs* (replacing *CEN15*) *TEL15R-tetOs TEL15L-tetOs TetR-GFP YFP-TUB1* P_{MET3}-*CDC20* cells (T3845) were treated in the same way, and YFP (tubulin; red) and GFP (*CEN, TELs* on chromosome XV; green) images were acquired.

(C) Tubulin signals extended from *CEN3* for a greater length, under a mild osmotic stress. T3828 cells were treated as in (B), but 1/10 volume of 1 M sorbitol was added immediately after transfer to glucose-containing medium. YFP (tubulin; red) and CFP (*CEN3*; green) images were acquired every 30 s (time 0, start of image acquisition). MT extensions from *CEN3* are shown in (i) a representative time-lapse sequence and (ii) selected images. See also Supplemental Experimental Procedures and Movie S1. See Figure S1 in Supplemental Information.

for initial interaction. Spindle pole MTs grow in various directions, searching for KTs (Kirschner and Mitchison, 1986). However, initial encounters happen more efficiently than would be expected from a random search-and-capture process (Wollman et al., 2005).

In vertebrate cells in which the nuclear envelope is broken down ("open mitosis"), a concentration gradient of RanGTP is formed around chromosomes and "guides" spindle pole MTs toward them (Carazo-Salas and Karsenti, 2003; Caudron et al., 2005). This mechanism is effective over a long range (~20 μm) (Athale et al., 2008), but not over shorter ranges (~1 μm), over which small molecules such as RanGTP are not able to make a substantial gradient due to their rapid diffusion. Moreover, in cells undergoing "closed mitosis," such as yeast, a RanGTP gradient is not formed during mitosis, as its concentration is uniformly high in the nucleus. Thus, other unknown mechanisms may facilitate initial KT interaction with spindle pole MTs, particularly over short distances.

In the budding yeast *Saccharomyces cerevisiae*, spindle pole bodies (SPBs: equivalent to centrosomes in metazoan cells) are embedded in the nuclear envelope, which remains intact during mitosis. Moreover, KTs are connected to SPBs by MTs through almost the entire cell cycle (Winey and O'Toole, 2001). However, KTs are disassembled upon centromere DNA replication during early S phase, allowing centromeres to detach from MTs and move away from spindle poles (Kitamura et al., 2007). KTs are reassembled after 1–3 min and, as in vertebrate cells, capture the lateral sides of spindle pole MTs (Tanaka et al., 2005). Our data suggest that before KT capture of spindle pole MTs, MTs are generated at KTs. We have investigated how these MTs are generated, their polarity, and the role they play in mitosis.

RESULTS

Microtubules Extend from Kinetochores prior to Their Interaction with Spindle Pole Microtubules

To address whether MTs are generated at KTs in budding yeast, we analyzed the process of KT reassembly and subsequent interaction with spindle pole MTs during S phase (which overlaps with mitosis; Kitamura et al., 2007). We found that, after KTs were reassembled but before they interacted with spindle pole MTs, tubulin signals (α-tubulin Tub1 fused with a yellow fluorescent protein [YFP]) were often associated with KT signals (Mtw1 and Ctf19 fused with a green fluorescent protein [GFP]) (Figure 1A). Such KT-associated tubulin signals were neither connected to a spindle pole nor a part of spindle pole MTs. In the majority of cases, the KT-associated tubulin showed punctate signals; however, in some cases, the signals extended for some length (see Figure 6B).

Because KTs rapidly (within 1–3 min) interacted with spindle pole MTs after their reassembly (Kitamura et al., 2007), it was difficult to characterize KT-associated tubulin in detail. To overcome this, we used an assay system in which we could delay the KT reassembly and displace a centromere further away from a spindle pole (see Figure S1A available online) (Tanaka et al., 2005). In this assay, we regulated the activity of a particular centromere (*CEN3*), which was labeled with adjacent insertion of *tet* operators, bound by a Tet repressor-cyan fluorescent protein (CFP) fusion protein. The *CEN3* was conditionally inactivated by transcription from the adjacently inserted *GAL1-10* promoter. Then, during metaphase arrest by Cdc20 depletion,

we reactivated *CEN3* by turning off the *GAL1-10* promoter, allowing KTs to reassemble (*CEN* reactivation assay). In many cells, during metaphase arrest, the nucleus became elongated due to occasional back-and-forth motions of the spindle, resulting in *CEN3* becoming located at some distance (up to 5–6 μm) from the spindle, on which other centromeres had already been caught (Tanaka et al., 2005). Because of this *CEN3* position, it generally took a longer time (4–8 min) for *CEN3* to interact with spindle pole MTs after KT reassembly, compared with the usual centromere interaction in early S phase. Under these conditions, most (>95%) of the free *CEN3*s became associated with punctate tubulin signals (visualized with YFP; Figure 1Bi) after *CEN3* reactivation, whereas other loci, such as telomeres on the same chromosome, did not (Figure 1Bii). In most cells, we observed the extension of tubulin signals from these punctate signals at *CEN3* (Figure 1Biii; Figure S1B).

The intensity of tubulin signals (per length) extending from *CEN3* was similar to that of spindle pole MTs (quantification not shown). We therefore interpreted this as MTs extending from KTs before they interacted with spindle pole MTs. Compared with spindle pole MTs, KT-derived MTs showed a similar growth rate, a higher shrinkage rate, and less frequent rescue events (conversion from shrinkage to growth) (Figure S1C).

In light of these findings, we considered that the punctate tubulin signals (with the light-microscope resolution; Figures 1A, 1Bi, and 1Bii), often found at KTs might be single or multiple short MTs that could subsequently grow out (Figure 1Biii). The punctate tubulin signals indeed contained a number of tubulin molecules sufficient to compose MTs longer than 50 nm (Figure S1D). Consistent with this notion, we also found short MTs that are not connected to a spindle pole during S phase, using electron tomography (Figure S1E). However, we cannot rule out that tubulin subunits are also present at some KTs without being polymerized into MTs.

Meanwhile, we also found that longer MTs (up to 4–5 μm) extended if cells were exposed to a mild osmotic stress (Figure 1Ci; Movie S1 and Figure S1Bii; see Supplemental Experimental Procedures). Sometimes two (Figure 1Cii) or more (data not shown) MTs extended from *CEN3*. In the subsequent sections, we applied a mild osmotic stress when we needed to analyze several long KT-derived MTs; however, the conclusions from these experiments were confirmed in the absence of an osmotic stress where possible (see below).

Kinetochore-Derived Microtubules Have Their Plus Ends Distal to Kinetochores

To determine the polarity of KT-derived MTs, we carried out three types of experiments, in which we used the *CEN* reactivation system and applied a mild osmotic stress (as in Figure 1C). First, we visualized Bik1 (ortholog of CLIP170 in vertebrates) with YFP, while *CEN3* and tubulins were visualized with CFP (Figure 2A). Bik1 is a member of MT plus end tracking proteins (+TIPs) and thus should localize at the plus ends of growing MTs (Akhmanova and Steinmetz, 2008). Bik1 was indeed found at the distal ends (i.e., the tips farthest from a spindle pole) of spindle pole MTs, which are known to be the plus ends (Winey and O'Toole, 2001). Importantly, when MTs extended from *CEN3*, Bik1 localized at their ends distal to it, but not at *CEN3* (Figure 2A). A similar result was obtained for shorter KT-derived MTs in the absence of an osmotic stress (data not shown). These results suggest that the KT-derived MTs have their plus ends distal to KTs.

Second, we visualized Kip3 (a kinesin-8 family member) by fusing it with GFP (Figure 2B). Kip3 moves along a MT toward its plus end in vitro, and this was also the case on spindle pole MTs in vivo (Gupta et al., 2006; Varga et al., 2006). We found that Kip3 moved along a KT-derived MT, toward the end distal to *CEN3*. This also suggests that the distal ends of kinetcohore-derived MTs are plus ends.

Third, we photobleached YFP-Tub1 signals at a small region on a KT-derived MT (Figure 2C). While the KT-derived MT was growing or shrinking, the distance between *CEN3* and the photobleached region did not considerably change. This suggests that polymerization and depolymerization of KT-derived MTs took place at the ends distal to *CEN3*, but not at the *CEN3*-proximal ends. Given that MT plus ends, but not minus ends, undergo polymerization in vivo (Dammermann et al., 2003), we conclude that the distal ends of KT-derived MTs are plus ends. Thus, all three of these experiments reinforce the conclusion that MTs are generated at KTs with distal plus ends.

After MTs had been generated at *CEN3*, *CEN3* remained at their minus ends in ~70% of cases. However, in the other ~30%, *CEN3* moved from the minus end to the lateral surface of the KT-derived MTs (Figure S2A). In a few cases, *CEN3* subsequently reached the vicinity of the plus ends of KT-derived MTs (Figure S2B), but never stayed there (see Discussion).

Stu2, but Not the γ-Tubulin Complex, Is Required for Generating Microtubules at Kinetochores

What factors facilitate the generation of MTs from KTs? To address this question, we looked at the roles of candidate regulators. The CBF3, Ctf19, Mtw1, and Ndc80 complexes (containing Ndc10, Okp1, Dsn1, and Spc24, respectively) are canonical KT components (Westermann et al., 2007), which are required for the initial KT interaction with the lateral surface of spindle pole MTs (Tanaka et al., 2005). On the other hand, the Dam1 complex is loaded on KTs after they interact with spindle pole MTs (Tanaka et al., 2007); the Ipl1 complex is not required for the initial interaction, but it is essential for the proper orientation of this attachment on the spindle (Tanaka et al., 2002). We also investigated MT regulators. The γ-tubulin complex, containing γ-tubulin (Tub4), Spc98, and Spc97, facilitates MT nucleation at spindle poles (Schiebel, 2000). +TIPs (Stu2, Bim1, and Bik1; orthologs of XMAP215/ch-TOG, EB1, and CLIP170, respectively, in vertebrates) localize at the plus ends of spindle pole MTs and facilitate their extension (Wolyniak et al., 2006 and references therein).

Using mutants, we quantified how frequently punctate tubulin signals appeared at *CEN3* after its reactivation but prior to its interaction with spindle pole MTs (Figure 3Aii; Figure S3A). We also quantified the frequency of MT extension from *CEN3* under a mild osmotic stress (Figure 3Aiii; Figure S3B). We assumed that these two measures reflected MT nucleation at *CEN3* and extension from it, respectively ("nucleation" is defined as the formation of very short MTs, from which MTs can further extend). As a control, we also studied MT extension from spindle poles (Figure 3Ai). We found that both the nucleation and extension of MTs from *CEN3* were defective in *ndc10-1*, *okp1-5*, *dsn1-7*,

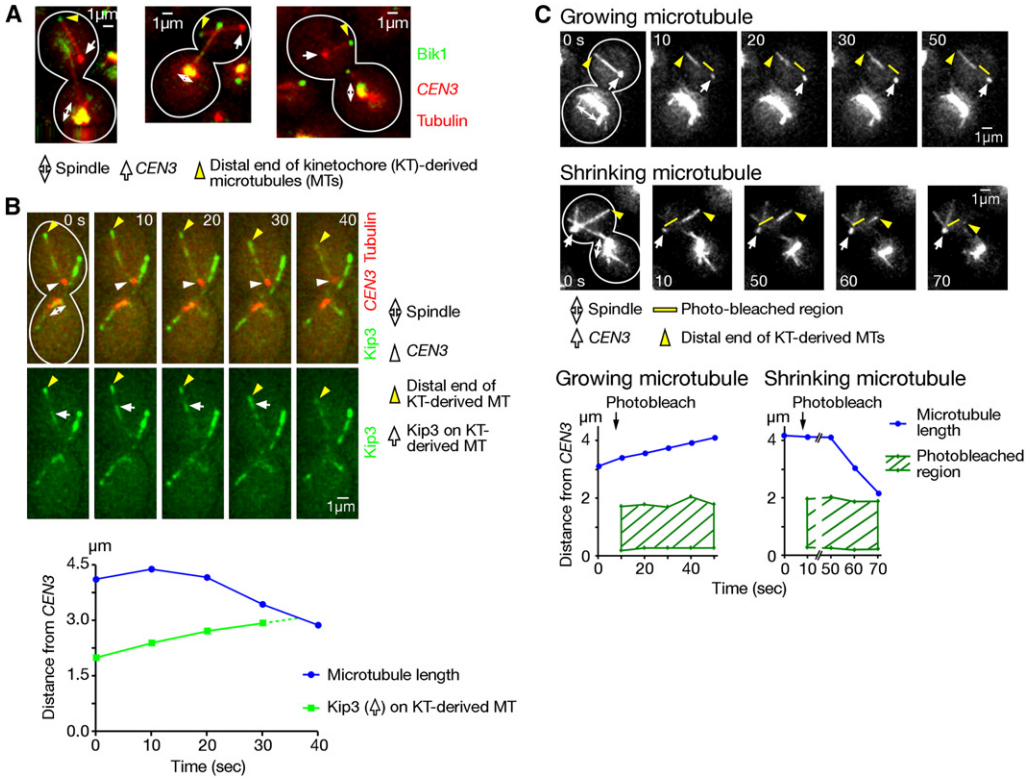

Figure 2. Kinetochore-Derived Microtubules Have Their Plus Ends Distal to Kinetochores

(A) Bik1 signals were found at the distal ends of KT-derived MTs, but not at *CEN3*. *PGAL-CEN3-tetOs TetR-3×CFP CFP-TUB1 BIK1-3×YFP PMET3-CDC20* cells (T3673) were treated as in Figure 1C. YFP (Bik1; green) and CFP (*CEN3*, tubulin; red) images were acquired.

(B) Kip3 moved along KT-derived MTs, heading toward the end distal to *CEN3*. *PGAL-CEN3-tetOs TetR-3×CFP CFP-TUB1 KIP3-3×GFP PMET3-CDC20* cells (T3981) were treated as in Figure 1C. GFP (Kip3; green) and CFP (*CEN3*, tubulin; red) images were acquired every 10 s (time 0, arbitrary). Representative time-lapse images (top) and graphs (bottom) showing the length of the relevant KT-derived MT as well as the position of a Kip3 signal (indicated by arrows in top panels) on it.

(C) Polymerization and depolymerization of KT-derived MTs occurred at the ends distal to *CEN3*. *PGAL-CEN3-tetOs TetR-GFP YFP-TUB1 PMET3-CDC20* cells (T3531) were treated as in Figure 1C. A small region, close to *CEN3*, on a KT-derived MT was photobleached between 0 and 10 s, while the KT-derived MT was either growing or shrinking (in five and six cells, respectively). YFP (tubulin) and GFP (*CEN3*) signals were acquired together every 10 s (time 0, arbitrary). Representative time-lapse images (top) and graphs (bottom) showing the length of the KT-derived MTs and the positions of the photobleached regions. Other cells showed similar results. See Figure S2 in Supplemental Information.

and *spc24-1* mutants (the result of *ndc10-1* is highlighted in Figure 3B), but not in *dam1-1* or *ipl1-321* mutants (Figures 3Aii and 3Aiii). Thus, canonical KT components are required for both the nucleation and extension of MTs from the KT.

On the other hand, *tub4-1* and *spc98-1* mutants did not show such defects (Figures 3Aii and 3Aiii), suggesting that the γ-tubulin complex is not required for generating KT-derived MTs. This notion was consistent with the additional finding that Tub4 and Spc97 (fused with GFPs) signals were found, with high intensity, at spindle poles, but not at *CEN3* (Figure S3C).

Intriguingly, in the *stu2-10* mutant, both the nucleation and extension of MTs from *CEN3* were defective (Figure 3C), whereas in *bim1*Δ and *bik1*Δ only the extension, but not the nucleation, was defective (Figures 3Aii and 3Aiii). Thus, Stu2 may be required for both the nucleation and extension, but Bim1 and Bik1 are required only for the extension. Consistent with this, Stu2 signals were found at *CEN3* before as well as after the appearance of punctate tubulin signals there (Figure 3D; Movie S2). Stu2 also localized at the plus ends of KT-derived MTs when they had extended from *CEN3*. By contrast, Bik1 and Bim1 were not found at *CEN3*, but were present at the plus ends of KT-derived MTs only after they began extending from *CEN3* (Figure S3D and Movie S3; data not shown).

As Stu2 localizes at *CEN3* before its interaction with spindle pole MTs, we next addressed if this localization is dependent on KT components. Stu2 localization at *CEN3* was abolished (or reduced) in mutants of canonical KT components, such as *ndc10-1*, *okp1-5*, *dsn1-7*, and *spc24-1*, but not in *dam1-1*, *ipl1-321*, *tub4-1*, *spc98-1*, or *bik1*Δ (Figure 3Aiv; Figure S3E). Intriguingly, this was the same subset of mutants that showed defects in the nucleation of MTs from KTs (Figure 3Aii). Whereas KT component mutants abolished Stu2 localization at *CEN3*, the *stu2-10* mutant did not impair the assembly of the KT components Mtw1 and Ndc80 (Figure 3C). These results raised the possibility that Stu2 may have a central role in the initial steps of generating MTs at KTs.

Stu2 Tethering at a Chromosome Arm Locus Is Sufficient to Generate Microtubules

The results reported above prompted us to test whether Stu2 is sufficient to nucleate and extend MTs if loaded on a chromosome. To test this, we engineered and tethered Stu2 proteins

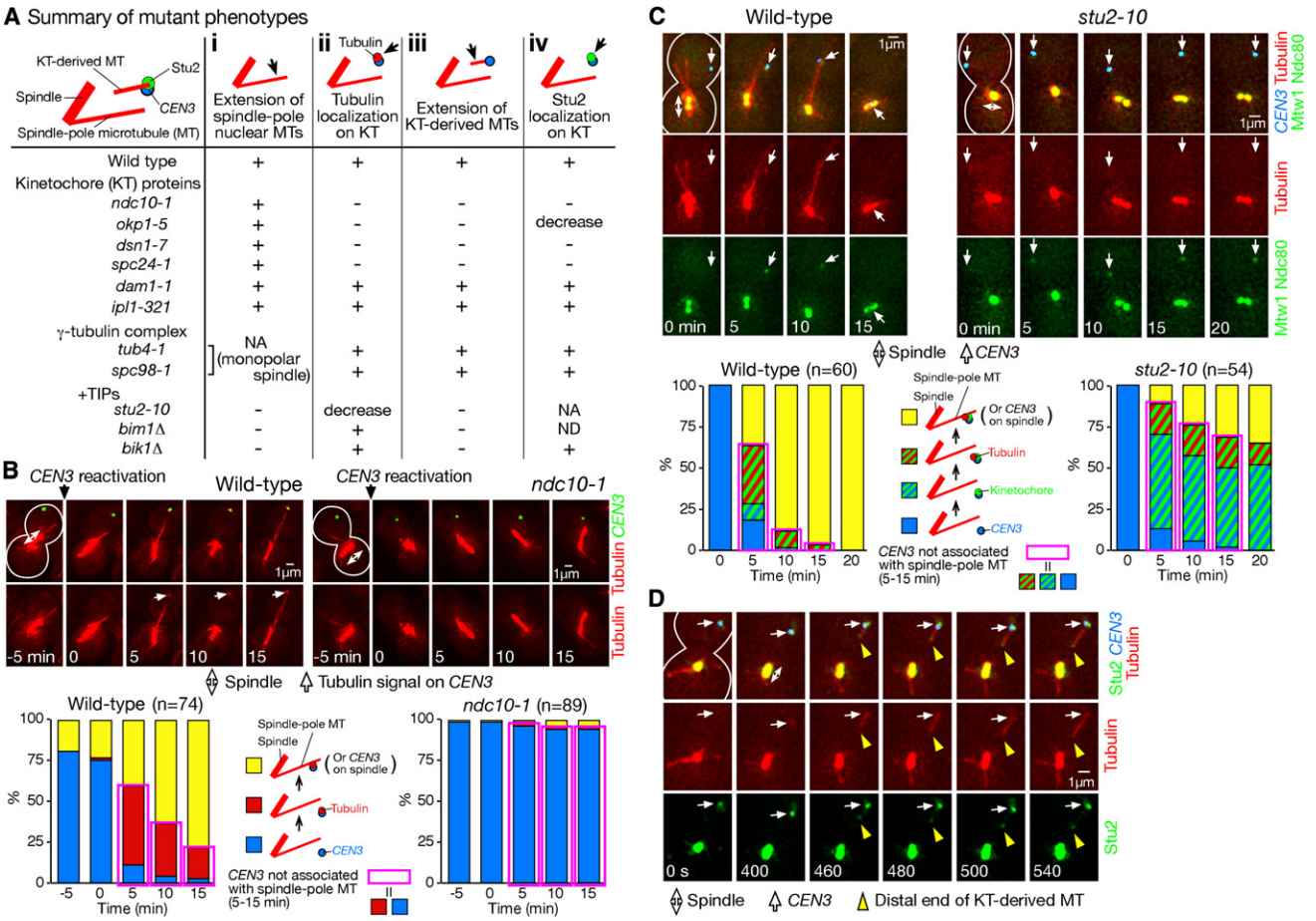

Figure 3. Kinetochore Components and +TIPs, but Not the γ-Tubulin Complex, Facilitate the Generation of Microtubules from Kinetochores

(A) Summary of mutant phenotypes. Using the *CEN* reactivation assay (Figure S1A), (i and iii) the extension of spindle pole and KT-derived MTs (original data, not shown and in Figure S3B, respectively) as well as (ii and iv) tubulin and Stu2 signals at KTs (original data in Figures S3A and S3E, respectively) were studied in wild-type and various mutant cells. NA, not applicable; ND, not determined.

(B) *ndc10-1* mutant cells were defective in the nucleation of MTs at KTs and *CEN3* interaction with spindle pole MTs. Wild-type *NDC10*$^{+}$ (T3828) and *ndc10-1* (T4230) cells with *P*$_{GAL}$*-CEN3-tetOs TetR-3×CFP YFP-TUB1 P*$_{MET3}$*-CDC20* were treated as in Figure 1B, but the temperature was raised to 35°C 30 min before cells were suspended in synthetic complete medium containing glucose and methionine. YFP (tubulin; red) and CFP (*CEN3*; green) images were acquired every 5 min at 35°C. Top: representative time-lapse images (time 0: transfer to glucose-containing medium). Bottom: changes in percentages of cells in which *CEN3* was (yellow) and was not (magenta) associated with spindle pole MTs. The latter cases were further divided into two, in which tubulin signals were found (red) or not (blue) at *CEN3*. n, number of observed cells.

(C) The *stu2-10* mutant was defective in the nucleation of MTs at *CEN3*, but showed normal KT reassembly. Wild-type *STU2*$^{+}$ (T6670) and *stu2-10* (T7285) cells with *P*$_{GAL}$*-CEN3-tetOs TetR-3×CFP YFP-TUB1 MTW1-4×mCherry NDC80-4×mCherry P*$_{MET3}$*-CDC20* were treated as in (B). mCherry (KTs; Mtw1, Ndc80; green), YFP (tubulin; red), and CFP (*CEN3*; blue) images were acquired every 5 min. Data are presented as in (B) (the presence of KT signals is shown in green stripes).

(D) Localization of Stu2 at *CEN3* and the plus ends of KT-derived MTs. *P*$_{GAL}$*-CEN3-tetOs TetR-3×CFP YFP-TUB1 STU2-4×mCherry P*$_{MET3}$*-CDC20* cells (T6987) were treated as in Figure 1C. mCherry (Stu2; green), YFP (tubulin; red), and CFP (*CEN3*; blue) images were acquired every 20 s (time 0; arbitrary). See also Movie S2. See Figure S3 in Supplemental Information.

at a chromosome arm locus, distant from a centromere. Stu2 was fused with GFP and a *lac* repressor, LacI, (Stu2-GFP-LacI), and tethered to an array of *lac* operators (*lacO*s) integrated on a chromosome arm locus (Figure 4A).

Stu2-GFP-LacI, but not a control construct, GFP-LacI, localized on the spindle (similarly to authentic Stu2); nonetheless, both showed accumulation at *lacO*s as expected (Figure 4B). Intriguingly, tubulin signals were associated with the GFP signal at *lacO*s after accumulation of Stu2-GFP-LacI, but not GFP-LacI, at *lacO*s (Figure 4B). These results were obtained not only in metaphase-arrested cells (Figure 4), but also in cells in early mitosis without arrest (data not shown). In several cells, the Stu2 signal at its tethered sites showed similar intensity to that at centromeres, but was still associated with tubulin signals (Figure S4A). Thus, tubulin signals at the Stu2-tethered site were not artifacts due to a higher accumulation of Stu2. Furthermore, tubulin signals at the Stu2-tethered site were not reduced in a *ndc10-1* (Figure S4B) or a *ndc80-1* mutant (data not shown), suggesting that they do not require canonical KT components.

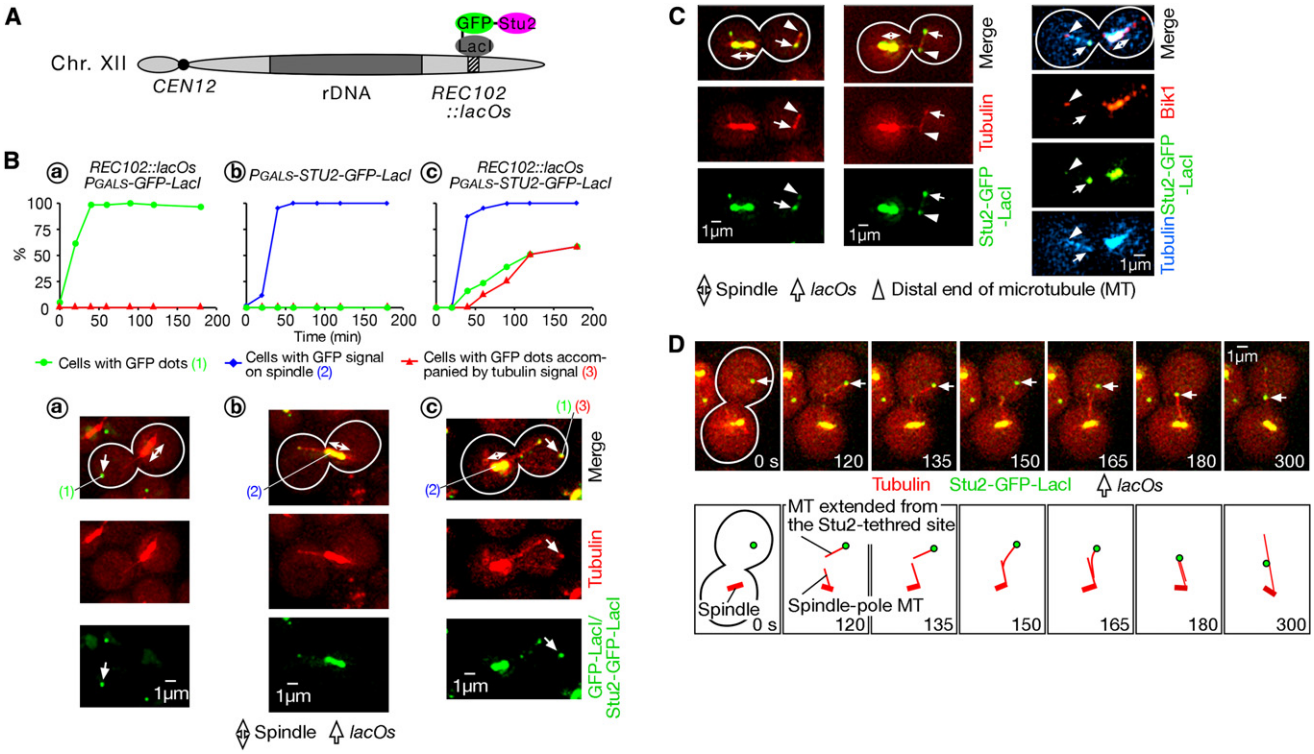

Figure 4. Stu2 Is Sufficient to Nucleate and Extend Microtubules when It Is Tethered on a Chromosome Arm Locus

(A) A schematic diagram of Stu2 tethering on a chromosome arm locus. See text for details.

(B) Tubulin signals were often found at the Stu2-tethered site. *PGALS-STU2-GFP-LacI REC102::lacOs CFP-TUB1 PMET3-CDC20* (T4837) cells were treated with α factor in methionine drop-out medium with raffinose for 2.5 hr, and then released to YP medium containing raffinose and 2 mM methionine. After 2.5 hr, galactose was added to the medium (time 0 in graphs). As controls, cells with *PGALS-GFP-LacI* instead of *PGALS-STU2-GFP-LacI* (T4601) and cells lacking *lacOs* (T4840) were treated in the same way. GFP (Stu2 fused with LacI or LacI alone; green) and CFP (tubulin; red) images were acquired at indicated time points. Percentages of cells in each category (top) and representative images (at 60 min in graphs: bottom) of T4601, T4840, and T4837 cells (left to right).

(C) MTs extended from the Stu2-tethered site with distal plus ends. T4837 cells (see [B]) were treated as in (B), except that 1/10 volume of 1 M sorbitol was added to medium immediately before GFP and CFP images were acquired (left). Cells (T7184) with the same genotype as T4837, but with *BIK1-4×mCherry*, were treated in the same way, followed by acquisition of mCherry (Bik1; red), GFP (Stu2 fused with LacI; green), and CFP (tubulin; blue) images (right).

(D) MTs, extended from the Stu2-tethered site, showed interaction with spindle pole MTs. T4837 cells (see [B]) were treated as in (C). GFP and CFP images were acquired every 15 s (time 0: start of image acquisition). Representative time-lapse images (top) and schematic diagrams (bottom). See also Movie S4. See Figure S4 in Supplemental Information.

When a mild osmotic stress was applied, MTs sometimes extended from the Stu2-tethered site (33%, 21/63; Figure 4C, left), but never from the GFP-LacI site. On such MTs, Bik1 (fused with monomer Cherry: mCherry) was detected at the MT ends distal to the Stu2-tethered site (Figure 4C, right), implying that the distal ends are plus ends, similar to KT-derived MTs.

Remarkably, in some cells (10%, 6/63), Stu2-tethered sites, with associated tubulin signals, interacted with spindle pole MTs and were subsequently transported toward a spindle pole (Figure S4C), albeit with frequent detachment from spindle pole MTs (data not shown). This was reminiscent of the transport of authentic centromeres toward a spindle pole by spindle pole MTs (Tanaka et al., 2007). Furthermore, similarly to MTs extending from *CEN3* (see Figure 5A), MTs extending from the Stu2-tethered site occasionally interacted with spindle pole MTs, which was followed by loading of the Stu2-tethered site on the lateral surface of spindle pole MTs (Figure 4D; Movie S4).

Altogether, we conclude that Stu2 is sufficient to nucleate and extend MTs when it is tethered at a chromosome arm locus. Stu2-tethered sites can recapitulate some features of authentic KTs, regarding the interaction with spindle pole MTs.

Kinetochore-Derived Microtubules Interact with Spindle Pole Microtubules, on which Kinetochores Are Subsequently Loaded

Do KT-derived MTs have a beneficial cellular role? To address this question, we examined events involving KT-derived MTs. After extension from a reactivated *CEN3* (as in Figure 1C), KT-derived MTs often interacted with spindle pole MTs (Figure 5A). After the initial encounter, they interacted with each other along their length, either in an antiparallel (Figure 5Ai; Movie S5) or parallel manner (Figure 5Aii; Movie S6); i.e., plus and minus ends point in the opposite and the same directions, respectively. In many cases, the interaction between the two types of MTs led to the loading of *CEN3* on the lateral surface of spindle pole MTs (Figure 5A); thus, KT-derived MTs may facilitate KT interaction with the lateral surface of spindle pole MTs. In other cases, *CEN3* seemed to be loaded first onto the spindle pole MTs,

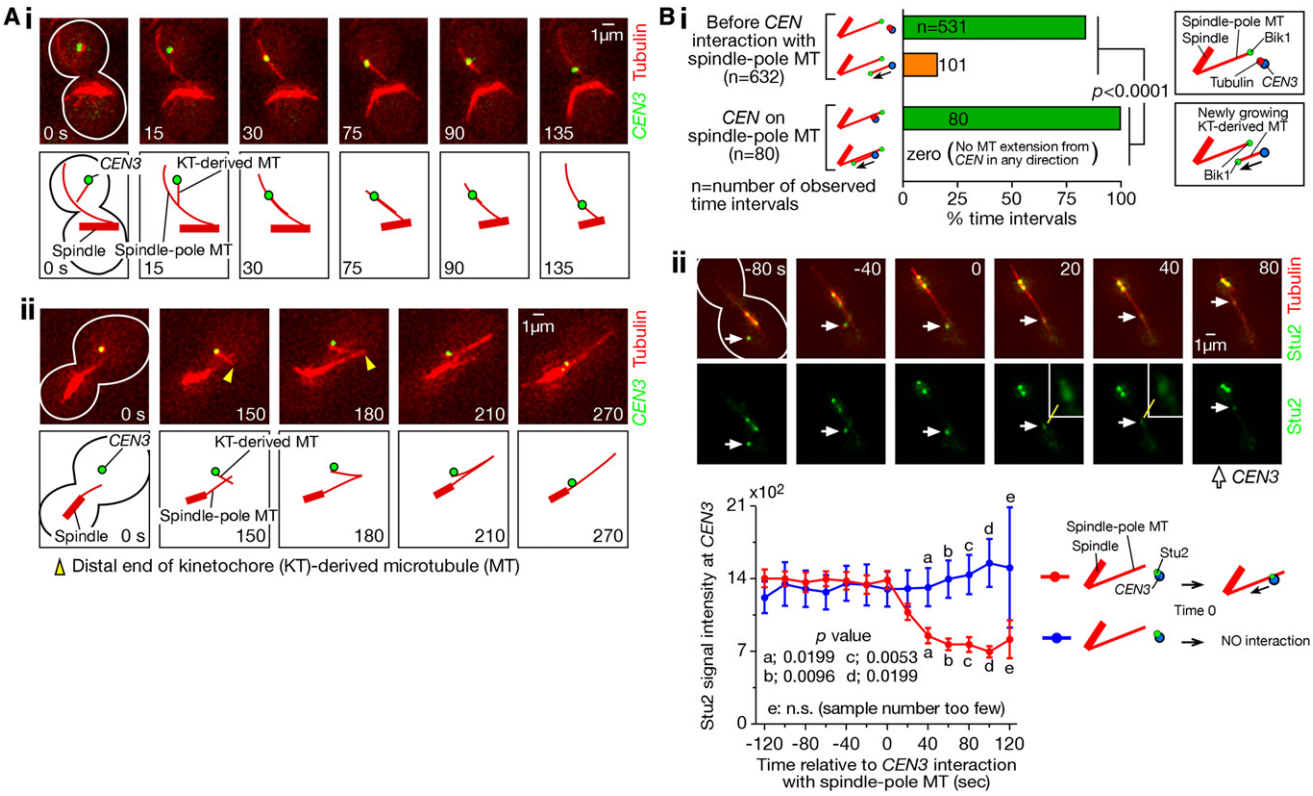

Figure 5. Kinetochore-Derived Microtubules Interact with Spindle Pole Microtubules, onto which Kinetochores Are Subsequently Loaded and Cease Generating Microtubules

(A) KT-derived MTs interacted with spindle pole MTs, on which KTs were subsequently loaded. T3828 cells (Figure 1B) were treated as in Figure 1C. Images were acquired every 15 s. Representative time-lapse images (top) and schematic diagrams (bottom), showing interaction between a KT-derived MT and a spindle pole MT in an (i) anti-parallel and (ii) parallel manner. See also Movies S5 and S6.

(B) (i) *BIK1-4×mCherry* (T6718) and (ii) *STU2-4×mCherry* (T6987) cells with P_{GAL}-*CEN3-tetOs TetR-3×CFP YFP-TUB1* P_{MET3}-*CDC20* were treated as in Figures 1C and 1B, respectively. Images were acquired (i) every 30 s for 35 min and (ii) every 20 s for 30 min. (i) MTs did not show new growth from KTs after KTs interacted with spindle pole MTs. Graphs show the percentages of time intervals, during which new MTs started extension from *CEN3* before and after *CEN3* association with spindle pole MTs. n, number of observed time intervals. (ii) The amount of Stu2 at *CEN3* decreased immediately after *CEN3* interacted with the surface of spindle pole MTs. Representative time-lapse images showing Stu2 signals at *CEN3* (arrows) in cells where *CEN3*s interacted with spindle pole MTs (top). The mean (and SEM) of quantified Stu2 signal intensity at *CEN3* from 8 such cells (red line, bottom). Time is shown relative to *CEN3* encounter with spindle pole MTs. As a control for each cell, Stu2 intensity was measured at the same time points in a neighboring cell, in which *CEN3* did not interact with spindle pole MTs (blue line). n.s., not significant. See Figure S5 in Supplemental Information.

followed by interaction between the two types of MTs (Figure S5A), in which case the MT interaction may help stabilize *CEN3* association with spindle pole MTs. Thus, the two types of MTs interacted with each other in various orientations; consistent with this, MT extension from *CEN3* did not show particular preference in its direction (data not shown).

Kinetochore-Derived Microtubules Disappear Quickly after Kinetochores Are Loaded onto Spindle Pole Microtubules

What happens to KT-derived MTs after KTs are loaded on spindle pole MTs? Do KTs still generate MTs? To address these questions, we sought to visualize new growth of MTs from *CEN3*, using the *CEN3* reactivation system. This type of growth could overlap with spindle pole MTs. To identify any such overlapping MTs, we visualized Bik1 (with mCherry), which localizes at the plus ends of growing MTs (see above). By following Bik1 signals, we could discern new growth of MTs from a spindle pole, even if they overlapped with MTs that extended earlier from the same spindle pole (Figure S5B). Similarly, we should be able to visualize new growth of MTs from *CEN3* with this assay even if it overlaps with spindle pole MTs. However, new MT growth from *CEN3* was very rare while *CEN3* was associated with spindle pole MTs (Figure 5Bi; Figure S5C). The MTs that had already extended from *CEN* shrank and disappeared soon after KTs interacted with spindle pole MTs (note that rescue of KT-derived MTs was infrequent and that their shrinkage rate was high; see Figure S1C).

How is new MT growth from KTs suppressed after KTs are loaded onto the surface of spindle pole MTs? Given the central role of Stu2 in generating MTs from KTs, we quantified the amount of Stu2 at *CEN3* before and after its interaction spindle pole MTs (Figure 5Bii; Figure S5D). Soon after *CEN3* had captured a spindle pole MT, there was a significant reduction in the Stu2 signal associated with it. How does this reduction happen? In many cases, immediately after *CEN3* was loaded

on a spindle pole MT, Stu2 signals seemed to disperse along a spindle pole MT toward both its plus and minus ends (insets in Figure 5Bii, 20 and 40 s). This finding is consistent with the observation that XMAP215 (Stu2 ortholog in *Xenopus*) shows diffusion along a MT in vitro (Brouhard et al., 2008). Stu2 reduction at *CEN3* at least partly explains how new MT growth from KTs is suppressed after they interact with spindle pole MTs.

Kinetochore-Derived Microtubules Appear More Frequently When Kinetochore Interaction with Spindle Pole Microtubules Is Delayed

Next, we investigated how KT-derived MTs are regulated physiologically during normal S phase (which overlaps with mitosis in budding yeast; Kitamura et al., 2007), i.e., without any artificial centromere regulation, cell cycle arrest, or an osmotic stress. After KTs were reassembled on centromeres after their disassembly and centromere detachment from MTs (Kitamura et al., 2007), punctate tubulin signals, presumably short MTs, appeared at KTs prior to their interaction with spindle pole MTs (in 39% cases, 29/75) (see Figure 6A); in some cells (12% of total, 9/75), we observed MT extension from KTs (see Figure 6B). Under the same condition, Bik1 also localized at the distal ends of MTs that extended from KTs (Figure S6A). In a *stu2-10* mutant, but not in *tub4-1* or *spc98-1* mutants, the MT/tubulin signals at KTs were reduced (Figure S6B). Thus, under physiological conditions, KT-derived MTs have their plus ends distal to KTs, and Stu2, but not the γ-tubulin complex, plays a pivotal role in generating MTs at KTs, consistent with the centromere reactivation assay.

Subsequently, again in physiological conditions, we examined the timing of the appearance of MTs/tubulins at KTs. We tracked each KT signal (Mtw1 and Ndc80) from its first appearance (i.e., reassembly after centromere DNA replication; defined as time 0) until its interaction with spindle pole MTs (Figures 6A and 6B). Figure 6A shows the time points (observed every 10 s) at which MT/tubulin signals (that were not connected to spindle pole MTs) were found at KTs (cyan box) in each event. The MT/tubulin signals appeared more frequently on KTs at later time points (Figures 6Ci and 6Cii), suggesting that they tended to appear at KTs when there was a delay in KT interaction with spindle pole MTs.

Evidence that Kinetochore-Derived Microtubules Facilitate Interaction between Kinetochores and Spindle Pole Microtubules

We sought to address whether KT-derived MTs facilitate the initial KT interaction with spindle pole MTs. However, we could not test this directly due to a lack of methods for inactivating MT generation, specifically at KTs, without affecting other KT functions or MT generation at spindle poles. We therefore used alternative approaches.

First, we investigated how the percentage of free KTs (i.e., ones not yet attached to spindle pole MTs) decreases over time. We used the data in Figure 6A and plotted the percentage against the time elapsed from the first appearance of KT signals (Figure 6D). These plots were very well fit by a simple exponential decay curve ($R^2 > 0.98$). Therefore, at any given time point, the expected time required for a free KT to interact with spindle pole MTs should always be constant and equal to the half life (43.7 s), featured in the curve (Figure 6D).

Next, we investigated whether there is a correlation between the appearance of MT/tubulin signals at KTs and their efficient interaction with spindle pole MTs. To test this, we plotted the percentage of free KTs similarly to the method used in Figure 6D, but against the time elapsed from the first appearance of MT/tubulin signals at the KT (Figures 6Ei and 6Eii). Compared with Figure 6D, the percentage of free KTs declined more rapidly after the first appearance of MT/tubulin signals for two or more consecutive time points (Figure 6Eii). This correlation does therefore seem to be present.

However, this correlation may not reflect a direct causal relationship. For example, KTs become more mature (e.g., accumulate more components) at later time points while they are not associated with spindle pole MTs, and this may have a more direct effect on KT capture by spindle pole MTs. The MT/tubulin signals at the KT might appear simply as a result of this KT maturation. To test this possibility, we identified time points at which KT signals became brighter (Figures 6A and 6B, orange dots). Consistent with our assumption that brighter KT signals reflect more mature KTs, they were found more frequently at later time points (Figures 6Ciii and 6Civ). They also showed a correlation with the appearance of MT/tubulin signals at the KT (Figure S6C). However, the appearance of brighter KT signals did not advance the timing of KT interaction with spindle pole MTs (Figures 6Eiii and 6Eiv). A corollary is that the appearance of MT/tubulin signals at KTs has a greater effect on facilitating KT interaction with spindle pole MTs than KT maturation might have.

DISCUSSION

MTs are generated not only at spindle poles, but also at KTs in early mitosis (Rieder, 2005). In this study, using budding yeast as a model organism, we describe evidence that, during early mitosis, MTs extend from KTs with distal plus ends (Figure 7). Our data suggest that, once generated, KT-derived MTs often interact with spindle pole MTs along their length, which may facilitate KT loading onto the lateral surface of spindle pole MTs. We found that when this loading is complete, the new generation of MTs at KTs is suppressed, and MTs already extended from KTs quickly disappear. Thus, KT-derived MTs do not develop into the MTs that connect KTs to spindle poles. Therefore, our findings do not conflict with the established understanding of the polarity of the KT-spindle pole MTs that form the metaphase spindle; as identified in various eukaryotes, their plus ends are always at KTs (McIntosh and Euteneuer, 1984).

Our data also suggest that Stu2 is a key regulator in the generation of MTs at KTs. Stu2 belongs to an evolutionarily conserved family of MT-binding proteins, which includes Dis1 and Alp14 in fission yeast, Zyg9 in *C. elegans*, Msps in *Drosophila*, XMAP215 in *Xenopus*, and ch-TOG in mammals (Ohkura et al., 2001). The conserved TOG domains of these proteins directly bind tubulins (Al-Bassam et al., 2006), and XMAP215 is able to polymerize MTs in vitro (Brouhard et al., 2008). These proteins regulate the dynamics of MTs at their plus ends and also have crucial roles in organizing MT minus ends at spindle poles (Cassimeris and Morabito, 2004; Usui et al., 2003). We found that Stu2 also localizes to both ends of KT-derived MTs, consistent with its roles at both ends of these MTs.

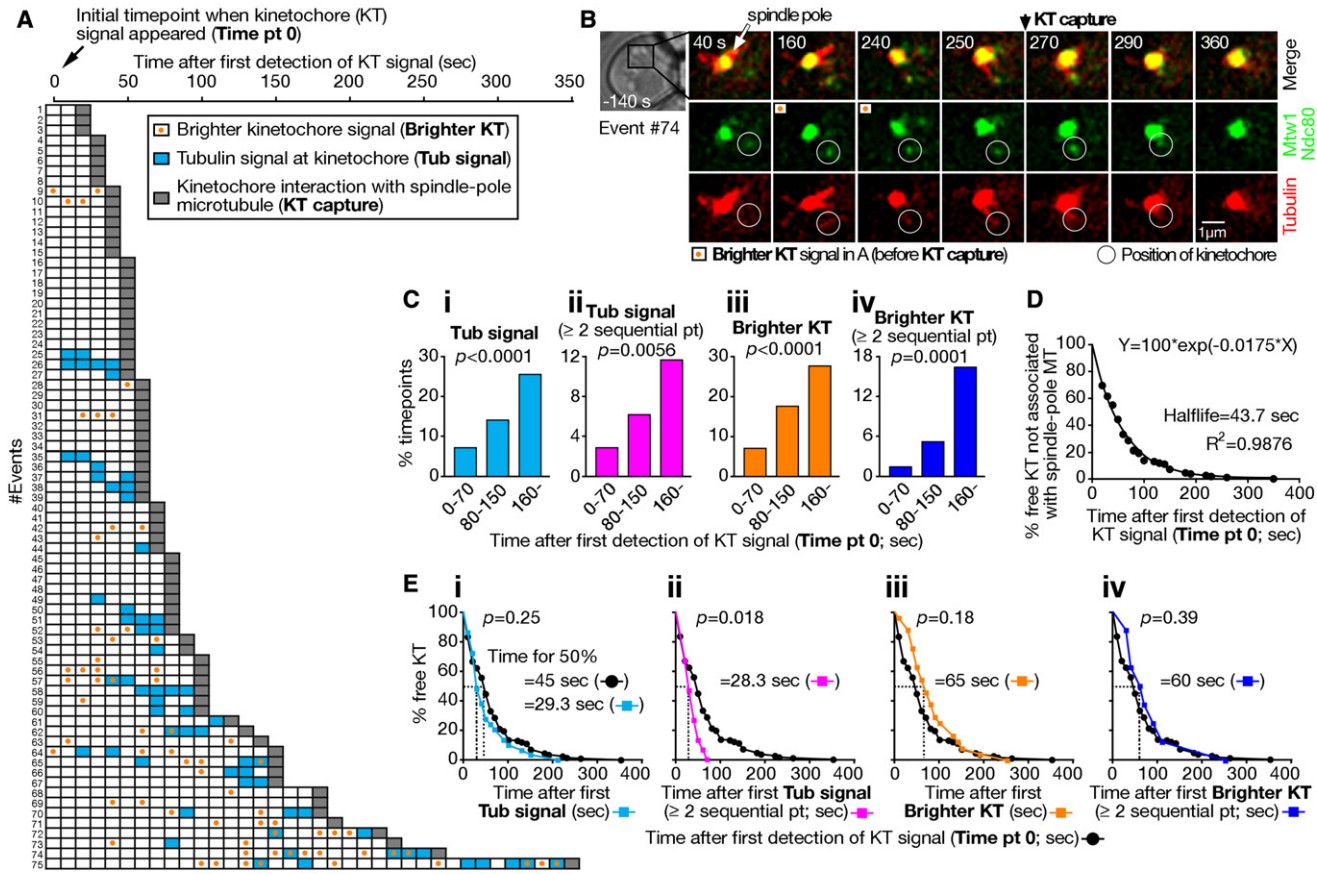

Figure 6. Kinetochore-Derived Microtubules Appear More Frequently When Kinetochore Interaction with Spindle Pole Microtubules Is Delayed, and then Seem to Facilitate This Interaction

(A–E) *MTW1-4×mCherry NDC80-4×mCherry YFP-TUB1* cells (T6444) were treated as in Figure 1A. From 20 min after washout of α factor, mCherry (KTs; green) and YFP (tubulin; red) images were collected every 10 s for 10 min. During this time window in S phase, KTs were often reassembled and reassociated with spindle pole MTs (Kitamura et al., 2007).

(A) Time points in each event (75 events from 71 cells), in which KT signals were detected (first detection at time 0) away from a spindle pole and subsequently interacted with spindle pole MTs (gray box). Time points showing KT-associated MT/tubulin signals (not connected to spindle pole MTs) are indicated by cyan boxes, whereas time points showing brighter KT signals are marked with orange dots.

(B) Representative time-lapse images (Event #74 in [A]) showing Mtw1-4×mCherry/Ndc80-4×mCherry signals in green and YFP-Tub1 in red. Time is shown in seconds (time 0 is as defined in [A]).

(C) Percentages of time points (in [A]) within each time window, showing (i) MT/tubulin signals at KTs (cyan) or (iii) brighter KT signals (orange), as well as those showing such signals for two or more consecutive time points (ii, magenta; iv, blue).

(D) Percentages of free KTs (shown in [A]), which were not yet associated with spindle pole MTs, are plotted (black dots) against the time after the first detection of KT signals (time 0 in [A]). A regression curve was drawn based on a one-phase exponential decay curve. The total number of free KTs at time 0 was predicted from this exponential decay curve, including those that escaped our observation due to a rapid interaction with spindle pole MTs after KT assembly (see Supplemental Experimental Procedures).

(E) Percentages of free KTs (shown in [A]) are plotted against the time (i) after the first appearance of MT/tubulin signals at KTs (cyan) and (ii) after their first appearance for two or more sequential points (time was measured from the first time point of consecutive ones: magenta). Percentages of free KTs are also plotted against the time (iii) after the first appearance of brighter KT signals (orange) and (iv) after their first appearance for two or more sequential points (blue). In each figure, a black line links the black dots shown in (D), providing a control for comparison with each colored line. See also Supplemental Experimental Procedures. See Figure S6 in Supplemental Information.

In contrast to our conclusion that KT-derived MTs have plus ends distal to KTs, previous reports with *Drosophila* cells suggested that KT-derived MTs have their plus ends at KTs and grow there by tubulin polymerization (Khodjakov et al., 2003; Maiato et al., 2004). How can this difference be reconciled? One possibility is that in both cases short MTs (perhaps 50–500 nm) are generated at KTs with plus ends distal to KTs (Witt et al., 1980). The minus ends of such short MTs are generally not embedded at KT plates in mammalian CHO cells (Witt et al., 1980) and indeed not tightly associated with KTs in budding yeast (see Figure S2). In budding yeast, these short MTs can grow further by tubulin polymerization at the distal plus ends. However, in fly cells (and perhaps in mammalian cells), the distal plus ends of the short KT-derived MTs might be captured by KT plates (polarity conversion) and grow by tubulin polymerization at KTs (Maiato et al., 2004).

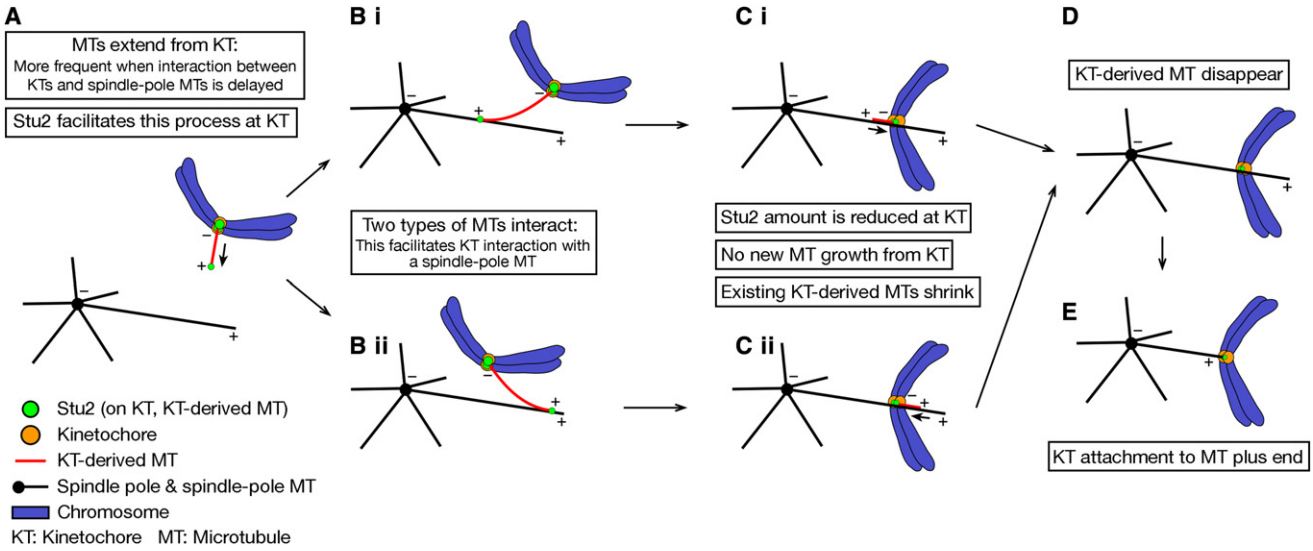

Figure 7. Summary of How Microtubules Are Generated at Kinetochores, How They Facilitate Kinetochore Interaction with Spindle Pole Microtubules, and How They Disappear Afterwards, in Budding Yeast

(A) MTs are generated at KTs with distal plus ends. Stu2 has a central role in promoting this process at KTs. This MT generation is more frequent when the KT interaction with spindle pole MTs is delayed.

(B) KT-derived MTs interact with spindle pole-derived MTs. This interaction takes place either in an (i) antiparallel or (ii) parallel manner, and facilitates KT loading onto the lateral side of spindle pole MTs.

(C and D) After KTs are loaded onto the lateral side of spindle pole MTs, the amount of Stu2 at KTs is reduced and new MT generation at KTs is suppressed. Existing KT-derived MTs shrink and quickly disappear.

(E) KTs subsequently attach to the distal plus ends of spindle pole MTs (Tanaka et al., 2007).

The polarity conversion of KT-derived MTs could be facilitated by a number of factors: (1) plus end-directed motors such as CENP-E localizing to KTs; (2) multiple binding sites of the MT plus ends on a single KT; and (3) the ability of KTs to polymerize MTs at their plus ends, which may be measured by the rate of MT flux (Rogers et al., 2005). Although all of these factors are vital in fly KTs (where MT flux rate is particularly high compared with other organisms; Rogers et al., 2005), KTs in budding yeast have no associated plus end-directed motors before interacting with spindle pole MTs (Tanaka et al., 2007), have only a single binding site of the MT plus ends (Winey et al., 1995), and show no MT flux (Maddox et al., 2000; Tanaka et al., 2005). In fact, even if KTs occasionally leave the minus ends of KT-derived MTs and associate with their lateral surface, they are not likely to reach and attach to the plus ends of these MTs (see Figure S2).

The polarity of KT-derived MTs in budding yeast agrees with that proposed in early studies with chromosomes isolated from CHO cells (Bergen et al., 1980; Summers and Kirschner, 1979). The conclusion in the early studies has remained controversial because it did not immediately fit the polarity of KT-spindle pole MTs in metaphase (see Introduction). Based on our current results, we propose that KTs may have the ability to nucleate MTs and subsequently organize the minus ends of KT-derived MTs in a wide range of cell types. The polarity of extending KT-derived MTs could be determined by multiple considerations such as cell type and stage in mitosis, which may influence the factors facilitating the polarity conversion (see above). For example, CENP-E is loaded at KTs during prometaphase (Yen et al., 1991), and the polarity conversion may occur more frequently in late prometaphase. Even in *Drosophila* cells, Msps (ortholog of Stu2) localizes at KTs (Buster et al., 2007) and, in certain conditions, may help generate MTs at KTs with distal plus ends.

Irrespective of their polarity, KT-derived MTs often interact with spindle pole MTs along their length (Khodjakov et al., 2003) (Figure 5A). However, depending on their polarity, the consequences of that interaction would differ. When KT-derived MTs have the minus ends distal to KTs, these distal ends are often collected by a spindle pole; thus, they develop into the MTs that link KTs to a spindle pole (Khodjakov et al., 2003). By contrast, KT-derived MTs with distal plus ends have a shorter lifetime and do not develop into KT-spindle pole MTs.

What factors mediate the interaction between KT-derived MTs (with distal plus ends) and spindle pole MTs along their length? One candidate is Ase1 (ortholog of PRC1 in vertebrates), which bridges antiparallel MTs during anaphase (Janson et al., 2007; Schuyler et al., 2003). We have preliminary evidence that Ase1 is detected when and where KT-derived MTs interact with spindle pole MTs in an antiparallel manner (unpublished data). However, *ase1*-deleted cells still showed this interaction, suggesting that there may be redundancy in terms of the mechanisms involved.

Our results also give insights into how spindle pole MTs might efficiently "locate" KTs for initial interaction; both spatial and temporal regulation would be involved. For spatial regulation, KT-derived MTs interact with spindle pole MTs, on which KTs are subsequently loaded (Figure 5A). We argue that KT-derived MTs can encounter spindle pole MTs more efficiently than can KTs without associated MTs. We provide evidence that the generation of KT-derived MTs shortens the time required for

KTs to be caught on spindle pole MTs. However, the degree to which KT-derived MTs with distal plus ends contribute to physiological mitosis will need to be determined through further testing. This mechanism would presumably be effective over a short range (<1–2 μm), given the length of KT-derived MTs in physiological conditions (Figure 6B). If a similar mechanism were effective in open mitosis, it could complement a long-range effect of a RanGTP gradient around chromosomes (see Introduction). For temporal regulation, we found that MTs are generated more often at KTs when KT interaction with spindle pole MTs is delayed. This may occur as KTs become more mature (presumably a larger number of KT components are assembled) while they remain unattached to the spindle. Thus, the generation of KT-derived MTs may help to avoid a further delay in the interaction with spindle pole MTs.

In this study, we have provided evidence that KTs nucleate MTs in vivo. Our data suggest that KT-derived MTs are abolished when KTs are loaded on the lateral surface of spindle pole MTs. Subsequently, KTs are tethered at the plus ends of spindle pole MTs (Figure 7), followed by sister KT biorientation on a metaphase spindle. Remarkably, KTs can organize minus ends of MTs during early mitosis, but then later attach to the plus ends of spindle pole MTs. During these processes, MT minus ends are associated only weakly with KTs, whereas the plus ends bind KTs robustly to resist tension, which is applied after biorientation is established. The stepwise development of the KT-MT interaction facilitates the initial interaction and subsequent biorientation on the spindle; both are crucial for proper chromosome segregation in the subsequent anaphase.

EXPERIMENTAL PROCEDURES

The background of yeast strains (W303) and methods for yeast culture were as described previously (Tanaka et al., 2007). Unless otherwise stated, cells were cultured at 25°C in YP medium containing glucose, and yeast genes were tagged at their C termini at their original gene loci by a one-step PCR method using 3×GFP-KanMX6 (pSM1023) (Maekawa et al., 2003) and 4×mCherry-NatMX6 (pT909) cassettes as PCR templates. The procedures for time-lapse fluorescence microscopy were described previously (Kitamura et al., 2007; Tanaka et al., 2007). Unless otherwise stated, time-lapse images were collected at 25°C. See more details in Supplemental Experimental Procedures.

SUPPLEMENTAL INFORMATION

Supplemental Information includes six figures, six movies, and Supplemental Experimental Procedures and can be found with this article online at doi:10.1016/j.devcel.2009.12.018.

ACKNOWLEDGMENTS

We thank L. Clayton, M. Renshaw, J.R. Swedlow, J.J. Blow, and members of the T.U.T. laboratory for discussions and reading the manuscript; C. Allan, S. Swift, and N. Kobayashi for technical help with microscopy and computing; K. Natsume and N. Kobayashi for technical help with yeast strain construction; S. Pruggnaller for help with electron tomography and analyses; R. Ciosk, F. Uhlmann, K. Nasmyth, D. Pellman, E. Schiebel, I.M. Cheeseman, G. Barnes, R. Tsien, S. Biggins, J. Lechner, K. Bloom, J.E. Haber, T. Hyman, A.W. Murray, A.F. Straight, J.V. Kilmartin, K.E. Sawin, T.N. Davis, M. Renshaw, European *Saccharomyces cerevisiae* Archive for Functional Analysis (EUROSCARF), and the Yeast Resource Centre for reagents. This work was supported by Cancer Research UK, the Medical Research Council, the Wellcome Trust, the Human Frontier Science Program, the Lister Research Institute Prize, and the Association for International Cancer Research. T.U.T. is a Senior Research Fellow of Cancer Research UK.

Received: June 21, 2009
Revised: October 28, 2009
Accepted: December 17, 2009
Published: February 15, 2010

REFERENCES

Akhmanova, A., and Steinmetz, M.O. (2008). Tracking the ends: a dynamic protein network controls the fate of microtubule tips. Nat. Rev. Mol. Cell Biol. *9*, 309–322.

Al-Bassam, J., van Breugel, M., Harrison, S.C., and Hyman, A. (2006). Stu2p binds tubulin and undergoes an open-to-closed conformational change. J. Cell Biol. *172*, 1009–1022.

Athale, C.A., Dinarina, A., Mora-Coral, M., Pugieux, C., Nedelec, F., and Karsenti, E. (2008). Regulation of microtubule dynamics by reaction cascades around chromosomes. Science *322*, 1243–1247.

Bergen, L.G., Kuriyama, R., and Borisy, G.G. (1980). Polarity of microtubules nucleated by centrosomes and chromosomes of Chinese hamster ovary cells in vitro. J. Cell Biol. *84*, 151–159.

Brouhard, G.J., Stear, J.H., Noetzel, T.L., Al-Bassam, J., Kinoshita, K., Harrison, S.C., Howard, J., and Hyman, A.A. (2008). XMAP215 is a processive microtubule polymerase. Cell *132*, 79–88.

Buster, D.W., Zhang, D., and Sharp, D.J. (2007). Poleward tubulin flux in spindles: regulation and function in mitotic cells. Mol. Biol. Cell *18*, 3094–3104.

Carazo-Salas, R.E., and Karsenti, E. (2003). Long-range communication between chromatin and microtubules in *Xenopus* egg extracts. Curr. Biol. *13*, 1728–1733.

Cassimeris, L., and Morabito, J. (2004). TOGp, the human homolog of XMAP215/Dis1, is required for centrosome integrity, spindle pole organization, and bipolar spindle assembly. Mol. Biol. Cell *15*, 1580–1590.

Caudron, M., Bunt, G., Bastiaens, P., and Karsenti, E. (2005). Spatial coordination of spindle assembly by chromosome-mediated signaling gradients. Science *309*, 1373–1376.

Dammermann, A., Desai, A., and Oegema, K. (2003). The minus end in sight. Curr. Biol. *13*, R614–R624.

Gupta, M.L., Jr., Carvalho, P., Roof, D.M., and Pellman, D. (2006). Plus end-specific depolymerase activity of Kip3, a kinesin-8 protein, explains its role in positioning the yeast mitotic spindle. Nat. Cell Biol. *8*, 913–923.

Howard, J., and Hyman, A.A. (2003). Dynamics and mechanics of the microtubule plus end. Nature *422*, 753–758.

Janson, M.E., Loughlin, R., Loiodice, I., Fu, C., Brunner, D., Nedelec, F.J., and Tran, P.T. (2007). Crosslinkers and motors organize dynamic microtubules to form stable bipolar arrays in fission yeast. Cell *128*, 357–368.

Khodjakov, A., Copenagle, L., Gordon, M.B., Compton, D.A., and Kapoor, T.M. (2003). Minus-end capture of preformed kinetochore fibers contributes to spindle morphogenesis. J. Cell Biol. *160*, 671–683.

Kirschner, M., and Mitchison, T. (1986). Beyond self-assembly: from microtubules to morphogenesis. Cell *45*, 329–342.

Kitamura, E., Tanaka, K., Kitamura, Y., and Tanaka, T.U. (2007). Kinetochore microtubule interaction during S phase in *Saccharomyces cerevisiae*. Genes Dev. *21*, 3319–3330.

Maddox, P.S., Bloom, K.S., and Salmon, E.D. (2000). The polarity and dynamics of microtubule assembly in the budding yeast *Saccharomyces cerevisiae*. Nat. Cell Biol. *2*, 36–41.

Maekawa, H., Usui, T., Knop, M., and Schiebel, E. (2003). Yeast Cdk1 translocates to the plus end of cytoplasmic microtubules to regulate bud cortex interactions. EMBO J. *22*, 438–449.

Maiato, H., Rieder, C.L., and Khodjakov, A. (2004). Kinetochore-driven formation of kinetochore fibers contributes to spindle assembly during animal mitosis. J. Cell Biol. *167*, 831–840.

McGill, M., and Brinkley, B.R. (1975). Human chromosomes and centrioles as nucleating sites for the in vitro assembly of microtubules from bovine brain tubulin. J. Cell Biol. *67*, 189–199.

McIntosh, J.R., and Euteneuer, U. (1984). Tubulin hooks as probes for microtubule polarity: an analysis of the method and an evaluation of data on microtubule polarity in the mitotic spindle. J. Cell Biol. *98*, 525–533.

Ohkura, H., Garcia, M.A., and Toda, T. (2001). Dis1/TOG universal microtubule adaptors - one MAP for all? J. Cell Sci. *114*, 3805–3812.

Rieder, C.L. (2005). Kinetochore fiber formation in animal somatic cells: dueling mechanisms come to a draw. Chromosoma *114*, 310–318.

Rieder, C.L., and Alexander, S.P. (1990). Kinetochores are transported poleward along a single astral microtubule during chromosome attachment to the spindle in newt lung cells. J. Cell Biol. *110*, 81–95.

Rogers, G.C., Rogers, S.L., and Sharp, D.J. (2005). Spindle microtubules in flux. J. Cell Sci. *118*, 1105–1116.

Schiebel, E. (2000). γ-tubulin complexes: binding to the centrosome, regulation and microtubule nucleation. Curr. Opin. Cell Biol. *12*, 113–118.

Schuyler, S.C., Liu, J.Y., and Pellman, D. (2003). The molecular function of Ase1p: evidence for a MAP-dependent midzone-specific spindle matrix. Microtubule-associated proteins. J. Cell Biol. *160*, 517–528.

Summers, K., and Kirschner, M.W. (1979). Characteristics of the polar assembly and disassembly of microtubules observed in vitro by darkfield light microscopy. J. Cell Biol. *83*, 205–217.

Tanaka, T.U. (2008). Bi-orienting chromosomes: acrobatics on the mitotic spindle. Chromosoma *117*, 521–533.

Tanaka, T.U., Rachidi, N., Janke, C., Pereira, G., Galova, M., Schiebel, E., Stark, M.J., and Nasmyth, K. (2002). Evidence that the Ipl1-Sli15 (Aurora kinase-INCENP) complex promotes chromosome bi-orientation by altering kinetochore-spindle pole connections. Cell *108*, 317–329.

Tanaka, K., Mukae, N., Dewar, H., van Breugel, M., James, E.K., Prescott, A.R., Antony, C., and Tanaka, T.U. (2005). Molecular mechanisms of kinetochore capture by spindle microtubules. Nature *434*, 987–994.

Tanaka, K., Kitamura, E., Kitamura, Y., and Tanaka, T.U. (2007). Molecular mechanisms of microtubule-dependent kinetochore transport toward spindle poles. J. Cell Biol. *178*, 269–281.

Usui, T., Maekawa, H., Pereira, G., and Schiebel, E. (2003). The XMAP215 homologue Stu2 at yeast spindle pole bodies regulates microtubule dynamics and anchorage. EMBO J. *22*, 4779–4793.

Varga, V., Helenius, J., Tanaka, K., Hyman, A.A., Tanaka, T.U., and Howard, J. (2006). Yeast kinesin-8 depolymerizes microtubules in a length-dependent manner. Nat. Cell Biol. *8*, 957–962.

Walczak, C.E., and Heald, R. (2008). Mechanisms of mitotic spindle assembly and function. Int. Rev. Cytol. *265*, 111–158.

Westermann, S., Drubin, D.G., and Barnes, G. (2007). Structures and functions of yeast kinetochore complexes. Annu. Rev. Biochem. *76*, 563–591.

Winey, M., and O'Toole, E.T. (2001). The spindle cycle in budding yeast. Nat. Cell Biol. *3*, E23–E27.

Winey, M., Mamay, C.L., O'Toole, E.T., Mastronarde, D.N., Giddings, T.H., Jr., McDonald, K.L., and McIntosh, J.R. (1995). Three-dimensional ultrastructural analysis of the *Saccharomyces cerevisiae* mitotic spindle. J. Cell Biol. *129*, 1601–1615.

Witt, P.L., Ris, H., and Borisy, G.G. (1980). Origin of kinetochore microtubules in Chinese hamster ovary cells. Chromosoma *81*, 483–505.

Wollman, R., Cytrynbaum, E.N., Jones, J.T., Meyer, T., Scholey, J.M., and Mogilner, A. (2005). Efficient chromosome capture requires a bias in the 'search-and-capture' process during mitotic-spindle assembly. Curr. Biol. *15*, 828–832.

Wolyniak, M.J., Blake-Hodek, K., Kosco, K., Hwang, E., You, L., and Huffaker, T.C. (2006). The regulation of microtubule dynamics in *Saccharomyces cerevisiae* by three interacting plus-end tracking proteins. Mol. Biol. Cell *17*, 2789–2798.

Yen, T.J., Compton, D.A., Wise, D., Zinkowski, R.P., Brinkley, B.R., Earnshaw, W.C., and Cleveland, D.W. (1991). CENP-E, a novel human centromere-associated protein required for progression from metaphase to anaphase. EMBO J. *10*, 1245–1254.